J Solid State Electrochem (2000) 4: 131–140

ORIGINAL PAPER

Jianhong Pei · Xiao-yuan Li

Preparation, characterization, and application of electrodes modified with electropolymerized one-dimensional Magnus' green salts: $Pt(NH_3)_4 \cdot PtCl_4$ and $Pt(NH_3)_4 \cdot PtCl_6$

Received: 22 April 1999 / Accepted: 30 June 1999

Abstract We report the modification of various electrode surfaces with electropolymerized Magnus' green salts, $[Pt(NH_3)_4 \cdot PtCl_4]_n$ and $[Pt(NH_3)_4 \cdot PtCl_6]_n$. The modified electrodes were prepared by cyclic scanning of the electrode potential in an aqueous solution containing $Pt(NH_3)_4^{2+}$ and $PtCl_4^{2-}$ or $PtCl_6^{2-}$ and the supporting electrolyte. The conditions for the film deposition were studied in detail. Several surface analytical techniques, including micro-Raman scattering and X-ray diffraction, were employed to characterize the modifier film. The electrochemical behavior of the modified electrode was studied in detail and the modified electrodes display very good electrocatalytic activity in the oxidation of ascorbic acid, hydrogen peroxide, thiosulfate, and especially nitric oxide.

Key words Chemically modified electrodes · Platinum ion complexes · Electropolymerization · Electrocatalysis · Magnus' green salts

Introduction

Electrodes modified with various electroactive molecules have found many applications in such fields as electroanalysis, electrocatalysis, photoelectrochemistry, energy storage, corrosion protection of metals, and electrochromic displays [1–4]. Much effort has been focused on a deeper understanding of the mechanism and kinetics, as well on as the fabrication of new systems, in addition to extensive exploration of their applications.

Chemically modified electrodes (CMEs) with various inorganic polymers, besides the ease in their preparation and fabrication, usually display excellent stability and specific reactivity. Inorganic polymers that contain chains of metal centers in their different oxidation states are of interest, not only for their good electronic conductivity but also for their inherent characteristics in chemical catalysis. Inorganic polymers that have been explored in the preparation of CMEs include polyoxometallates [5, 6], metalloporphyrins and related compounds [7–9], metal oxides [10–13] and polynuclear transition metal hexacyanometallates [14–22]. Among these, Prussian blue (PB) and its analogous compounds form stable and insoluble mixed valence films on the electrode surface, and have been widely studied [14–22]. The basic structure of the PB modifier film is a three-dimensional polymeric network consisting of alternating ferric and ferrous ions on cubic lattice sites. The ferric ions are coordinated to the nitrogen atoms, and the ferrous ions to the carbon atoms, of the bridging cyanide ligands [15, 20–22]. Although PB and its analogues can serve as effective charge distributors when used as modifiers on the electrode surface, the general lack of potent catalytic capability seriously limited their use in practical applications [5, 23]. This has compelled us to examine the potential of other inorganic conductive polymers as electrode modifiers, with the aim of not only retaining the modifier's role as an efficient electron mediator, but also adding to the mediator the desired catalytic capability. Magnus' green salts (MGS, platinum ion complexes) and their various analogues are a family of very attractive candidates to serve our goal for several reasons. First of all, to the best of our knowledge, they have received little attention so far in the use as electrode modifiers. Secondly, they are anticipated to be good electron mediators/distributors due to the well-defined Pt^{4+}/Pt^{2+} redox couple. Thirdly, Pt and its various ion complexes have documented and well-established catalytic behavior. Last, but not the least, MGS are a class

J. Pei (✉)[1]
Department of Inorganic,
Analytical and Applied Chemistry, Science II,
The University of Geneva,
30 Quai E. Ansermet, CH-1211 Geneva 4, Switzerland
e-mail: jianhong.pei@cabe.unige.ch

X. Li
Department of Chemistry,
The Hong Kong University of Science and Technology,
Clear Water Bay, Kowloon, Hong Kong

[1]On leave from Department of Chemistry,
The Hong Kong University of Science & Technology

of inorganic conductive polymers which have been used extensively in optical and electronic devices [24–28].

MGS complexes are usually of a one-dimensional structure in the solid state [24]. They can be grouped into two classes: complexes containing platinum in the same oxidation state (or type-I) and complexes composed of platinum in different oxidation states (or type-II). The structures of these two types of complex are shown in Fig. 1 [24]. The type-I structure comprises alternating dianions and dications in which two adjacent Pt ions are connected to each other directly through a metal-metal bond formed by the overlap of their d_z^2 orbitals. The type-II structure is formed by alternating square-planar d^8 Pt^{2+} complexes and octahedral d^6 Pt^{4+} complexes, connected by halogen bridges [24]. These one-dimensional inorganic polymers were prepared traditionally by slow solvent evaporation of a saturated solution [24, 29, 30]. An electrocystallization method has also been reported to provide crystals of these polymers [28, 31, 32]. The strong interest in these one-dimensional materials lies in a number of observations about their unusual anisotropic physical properties and chemical properties.

We have recently reported the preparation, characterization, and electrocatalytic applications of electrodes modified with electropolymerized $[CuPtCl_4 \cdot CuPtCl_6]_n$ [33]. The present work is a continuation of our study of novel inorganic films that can be electropolymerized onto the electrode surface. In this paper, we present the preparation, characterization, and electrocatalytic applications of electrodes modified by electropolymerized MGS, $[Pt(NH_3)_4 \cdot PtCl_4]_n$ and $[Pt(NH_3)_4 \cdot PtCl_6]_n$. The electrochemical properties of these CMEs and their potential applications in electroanalysis are systematically studied.

Experimental

Chemicals

Analytical grade K_2PtCl_4, K_2PtCl_6, and $Pt(NH_3)_4Cl_2$ as well as other chemicals were all from Aldrich and were used as received. The solutions were prepared by dissolving a definite amount of the chemicals in "triply distilled" water (deionized water followed by double distillation).

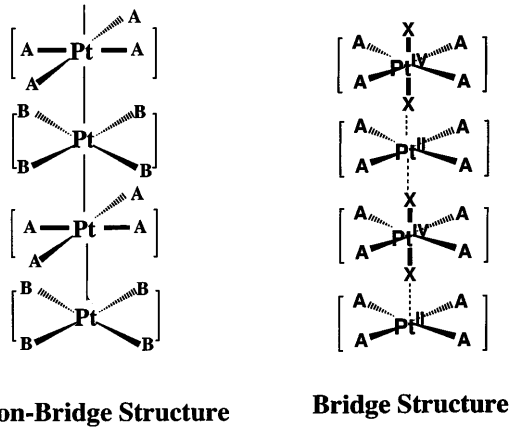

Fig. 1 Schematic drawings of typical structures for the one-dimensional platinum complexes: type 1, non-bridged structure (*left*); type 2, bridged structure (*right*)

Electrochemical measurements

All electrochemical measurements and the electrode modification were carried out on a BAS 100 B/W electrochemical workstation (Bioanalytical System, USA) controlled by the BAS 100 B/W software through a personal computer. The conventional three-electrode system was employed and a glassy carbon (GC) electrode (Φ3 mm, BAS) modified with $Pt(NH_3)_4 \cdot PtCl_4$ or $Pt(NH_3)_4 \cdot PtCl_6$ was used as the working electrode, with a platinum wire as the counter electrode, and SCE as the reference electrode. A 10-ml single-compartment glass vial with a Teflon cap was used as the electrochemical cell. The whole electrochemical cell was placed inside a BAS C-2 Faraday cage to avoid external interference. Except for the cases stated otherwise, all solutions were deaerated with pure nitrogen gas for at least 10 min prior to the electrochemical measurements and a nitrogen gas atmosphere was maintained over the solution during the measurements. All measurements were carried out at room temperature (~22 °C) and the potentials referred to the SCE. Prior to the electrochemical modification, the GC substrate electrode was treated by the following steps: polished with 0.05 μm alumina powder, rinsed with water, then placed in an ultrasonic cleaner for 5 min in 1 M HNO_3 and 10 min in water in sequence, polished again with 0.05 μm alumina, then cleaned in an ultrasonic cleaner for another 15 min in triply distilled water.

Electrode preparation

The $Pt(NH_3)_4 \cdot PtCl_6$ modified electrode was obtained by the continuous cyclic scanning of the potential at the working electrode (GC) in the modification solution from 700 mV to −800 mV (vs. SCE) at a scan rate of 100 mV/s. Typically, the modification solution contained 2.5×10^{-3} M $Pt(NH_3)_4Cl_2$, 2.5×10^{-3} M K_2PtCl_6, and 1 M KCl. When K_2PtCl_4 was used instead of K_2PtCl_6 in the modification solution, a $Pt(NH_3)_4 \cdot PtCl_4$ modified electrode was obtained. Usually 25 scans were taken in the preparation of the CMEs. The electrodes modified with MGS were rinsed thoroughly with the triply distilled water. Freshly prepared and deaerated modification solution is recommended, because some green solids were observable at the bottom of the solutions after they were left open to the air for several hours.

X-ray powder diffraction analysis

X-ray diffraction (XRD) patterns were obtained directly from the film on the electrode surface using a model MPD-18801 diffractometer (Philips, Netherlands). Reflections were recorded over a range of $10° < 2\theta < 50°$ at a speed of 0.01°/s. The Cu K_α radiation (1.5405 Å) was used in the measurement. The films for XRD measurements were prepared by continuous cyclic scanning of the potential at the working electrode in the modification solution with 25 scans at 10 mV/s in order to obtain a thicker and more uniform film on the electrode surface. The CME thus prepared displayed the same electrochemical behavior as that prepared using a scan rate of 100 mV/s.

Raman spectroscopy

Raman spectra were obtained on a MicroRaman/Photoluminescence System (model 3000, Renishaw, UK) with the 632.8 nm line of a HeNe laser as the excitation. The film was prepared on the surface of a platinum substrate (Φ 2 mm) to avoid the strong

Raman peak of the glassy carbon at $\sim$500 cm^{-1}, which interferes seriously with the Raman peaks of the modifier film. The film prepared on a Pt substrate displayed the same XRD pattern and electrochemical behavior as that prepared on a GC substrate.

Results and discussion

Preparation of the modified electrodes

Traditionally, MGS and its analogues were prepared by the slow evaporation of the solvent from their saturated solutions [29, 30]. Sometimes, the diffusion of the MGS complex through a membrane was used [30, 34]. These methods, despite the fact that they can offer good films or crystals, are usually quite slow. The electrodeposition method, on the other hand, has many advantages. For example, it allows the growth of a one-dimensional structure being achieved in a highly controllable manner and at a faster rate. It is also a chemically clean process in which indirect chemicals such as oxidizing agents can be avoided. The preparations of other inorganic films and crystals using electrochemical methods have been reported previously [31, 32, 35]. In the present work, the $Pt(NH_3)_4 \cdot PtCl_6$ film was polymerized on the surface of a GC electrode via continuous cyclic scanning of the potential at the working electrode in the solution containing 2.5×10^{-3} M $Pt(NH_3)_4Cl_2$ + 2.5×10^{-3} M K_2PtCl_6 + 1 M KCl. The potential was scanned from 700 mV to −800 mV (vs. SCE) at a rate of 100 mV/s. After several scans, it was already clearly visible that a film was formed on the electrode surface. We also found that, under the same conditions, the $Pt(NH_3)_4 \cdot PtCl_6$ film can also be electrodeposited on Pt and Au substrates. Thus, modified Pt and Au electrodes display identical electrochemical characteristics to the modified GC electrode. Therefore, no substrate-specific interaction exists between the $Pt(NH_3)_4 \cdot PtCl_6$ film and the substrate materials, and the substrate materials have no influence on the electrochemical response characteristics of the modified electrode. Indeed, the electrochemical characteristics of the modified electrode are decided by the modifier film itself. A film was also electrodeposited successfully on the electrode surface when K_2PtCl_4 was used as the anion supplier instead of K_2PtCl_6 in the modification solution. The electrode modified with $Pt(NH_3)_4 \cdot PtCl_4$ displays the same electrochemical characteristics as that modified with $Pt(NH_3)_4 \cdot PtCl_6$. The XRD study, however, revealed that the structures of the two films were actually different (vide infra).

Various other supporting electrolytes, such as KNO_3, K_2SO_4, Na_2SO_4, NaCl, and $MgSO_4$, were used to replace KCl in the modification solution, and the same results were obtained. This suggests that KCl in the modification solution only acts as a supporting electrolyte and does not take part in the film formation during the modification. It also indicates that the basic structures of the anion complex $PtCl_4^{2-}$ or $PtCl_6^{2-}$ remain unchanged during the film formation. If $PtCl_4^{2-}$ was changed into $PtCl_6^{2-}$ or vice versa during the film deposition, it is expected that the change of anions in the supporting electrolyte solution would affect the film deposition. The $Pt(NH_3)_4 \cdot PtCl_6$ and $Pt(NH_3)_4 \cdot PtCl_4$ films are naturally of the type-II and type-I structures, respectively, as shown in Fig. 1. As will be shown in the following, the XRD patterns of the two films support this conclusion. Some green solids appeared in the modification solution if it was placed open to the air for several hours; the green solids are the monomeric Magnus' green salts, precipitated as the ion-adduction compound. Although the detailed mechanism of the film growth on the electrode is not yet clear, it is likely that the polarization effect during cyclic scanning of electrode induced and facilitated the growth of the alternative layers of cation and anion along the stacking axis.

The $Pt(NH_3)_4 \cdot PtCl_6$ and $Pt(NH_3)_4 \cdot PtCl_4$ films can also be formed on the working electrode by galvanostatic and potentiostatic methods. When the GC electrode was immersed into the modification solution and its potential was kept at −800 mV for several minutes, green crystals were observed on the electrode surface. The potentiostatic method can also be used to prepare the crystals of Magnus' green salts on the substrate electrode. The crystals prepared by this method, however, do not strongly adhere to the electrode surface, making the CME unstable and less usable in analytical applications. Continuous cyclic scanning of the potential at the working electrode in the modification solution can give rise to a more uniform and more mechanically stable film. Therefore, the cyclic scanning method is adopted for the preparation of the modified electrodes in the work described in this paper.

Since both modified films, $[Pt(NH_3)_4 \cdot PtCl_6]_n$ and $[Pt(NH_3)_4 \cdot PtCl_4]_n$, display similar electrochemical properties, we will focus on the results obtained on the $Pt(NH_3)_4 \cdot PtCl_6$ modified electrode except for the cases stated otherwise. We will use MGSI/GC to denote the electrode modified with $Pt(NH_3)_4 \cdot PtCl_4$ (which has a type-I structure), and MGSII/GC to denote the electrode modified with $Pt(NH_3)_4 \cdot PtCl_6$ (which has a type-II structure).

Characterization

Raman spectra

Raman spectroscopy is a very useful tool to obtain structure information about the film. The ex situ Raman measurements were carried out on the $Pt(NH_3)_4 \cdot PtCl_6$ film electrodeposited on a Pt substrate electrode and typical results are shown in Fig. 2. The reason for using a Pt substrate instead of the GC substrate is because the GC itself has a very strong Raman scattering peak at $\sim$500 cm^{-1} which interferes with the signals from the film. In Fig. 2 the Raman peak at 337 cm^{-1} is readily assigned to the stretch vibration of Pt-Cl, in agreement with the literature [36, 37] and our diagnostic experiment

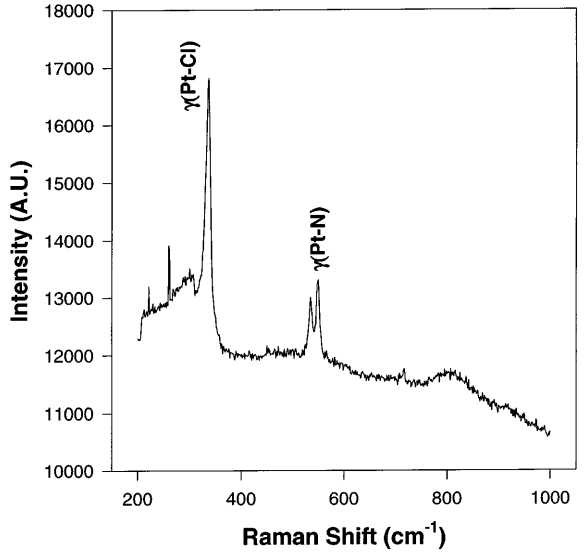

Fig. 2 Raman spectrum of $[Pt(NH_3)_4{\cdot}PtCl_6]_n$ film on a Pt substrate. Light source: 632.8 nm; exposure time: 1000 s; power: 3 mW

obtained on the solid powder of K_2PtCl_6. The Raman spectrum of the K_2PtCl_6 solid displays two bands in this region, at 319 cm^{-1} and 348 cm^{-1}, in contrast to the one strong and broad peak centered at 337 cm^{-1} obtained for the deposited film. This observation suggests that the equatorial and axial Pt-Cl bonds of the $PtCl_6^{2-}$ anion in the film are of similar strength. The two peaks at 535 cm^{-1} and 549 cm^{-1} are attributed to the stretching vibrations of the Pt-N bond, consistent with our diagnostic experiment obtained on the solid powder of $Pt(NH_3)_4Cl_2$, which displays two Pt-N Raman bands at 521 cm^{-1} and 537 cm^{-1}. They are also consistent with the literature data on the Raman frequency of the Pt-N bond [37, 38]. The upshift of the Pt-N stretching modes in the film indicates that the local environment of the $Pt(NH_3)_4^{2+}$ cation in the film, likely to be more compressed, is quite different from that in the ion-adduction solid. The Raman peak at 261 cm^{-1} can be assigned to the bending vibration of N-Pt-N [38]. The Raman results confirm the structure of the film as shown in Fig. 1.

X-ray diffraction

Figure 3 shows the XRD patterns of the $Pt(NH_3)_4 \cdot PtCl_4$ (curve 1) and the $Pt(NH_3)_4 \cdot PtCl_6$ (curve 2) films. The dominant diffraction peak of the $Pt(NH_3)_4 \cdot PtCl_4$ film appears at a 2θ value of 14.11°, corresponding to $d = 6.26$ Å, ($n\lambda = 2d\sin\theta$). The main diffraction peak of the $Pt(NH_3)_4 \cdot PtCl_6$ film appears at a 2θ value of 16.41°, corresponding to $d = 5.40$ Å. The main diffraction lines (diffraction depace) of the $Pt(NH_3)_4 \cdot PtCl_4$ powder [39] and the two films are listed in Table 1. It was reported that $Pt(NH_3)_4 \cdot PtCl_4$ crystallizes in a tetragonal system with unit cell constants $a = b = 6.3$ Å, $c = 5.26$ Å, and $\alpha = \beta = \tau = 90°$ [39]. The $Pt(NH_3)_4 \cdot PtCl_4$ film gave rise to sharp diffraction

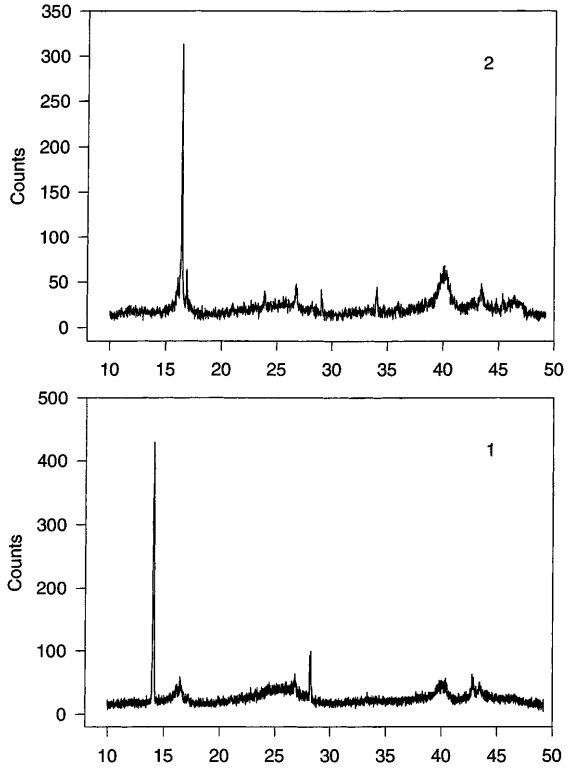

Fig. 3 The X-ray diffraction patterns of $[Pt(NH_3)_4{\cdot}PtCl_4]_n$ film (*1*) and $[Pt(NH_3)_4{\cdot}PtCl_6]_n$ film (*2*). Step: 0.01°; speed: 0.01°/min; wavelength: 1.5406 Å (Cu K_α)

lines at $d = 6.26$, 3.15, 2.11 Å, correlating very well with the (h00) reflections of $Pt(NH_3)_4 \cdot PtCl_4$ powder. In addition, the film gave rise to another diffraction line at $d = 5.38$ Å, and some other weak and broad diffraction lines. The diffraction peak at $d = 5.38$ Å, which did not appear in the $Pt(NH_3)_4 \cdot PtCl_4$ powder pattern, is probably contributed from a minor component of

Table 1 X-ray diffraction lines of $Pt(NH_3)_4{\cdot}PtCl_4$ powder and $Pt(NH_3)_4{\cdot}PtCl_4$ (1) and $Pt(NH_3)_4{\cdot}PtCl_6$ films (2) electrodeposited on a glassy carbon electrode

hkl	Powder	Diffraction	
		Film 1 (2θ)	Film 2 (2θ)
100	6.26	6.26 (14.11)	–
	–	5.38 (16.46)	5.40 (16.41)
	–	–	5.25 (16.87)
110	4.45	–	–
101	3.97	–	–
	–	–	3.72 (23.89)
	–	–	3.33 (26.74)
200	3.12	3.15 (28.20)	–
	–	–	3.07 (29.03)
210	2.81	–	–
002	2.64	–	2.63 (34.04)
102	2.41	–	–
220	2.22	–	2.25 (40.10)
300	2.11	2.11 (42.78)	2.08 (43.44)
310	1.98	–	–
410	1.52	–	–

$Pt(NH_3)_4 \cdot PtCl_6$ mixed in the film. The $Pt(NH_3)_4 \cdot PtCl_6$ film displays a completely different XRD pattern from that of the $Pt(NH_3)_4 \cdot PtCl_4$ film. Since the standard XRD data for $Pt(NH_3)_4 \cdot PtCl_6$ powder is not available, we are unable to establish the diffraction lines of the $Pt(NH_3)_4 \cdot PtCl_6$ film. However, from the diffraction patterns of the two films it is clear that the components of the two films are different, although they display remarkable similar electrochemical properties.

From the very sharp and very intense (100) diffraction at $d = 6.26$ Å for the $Pt(NH_3)_4 \cdot PtCl_4$ film and $d = 5.40$ Å for the $Pt(NH_3)_4 \cdot PtCl_6$ film, it is reasonable to conclude that the films were electrodeposited on the electrode surface with a preferred orientation. For the $Pt(NH_3)_4 \cdot PtCl_4$ film, the (100), (200), and (300) diffraction lines dominate the XRD pattern, indicating that the complexes in the film are arranged mainly along the stacking axis (see Fig. 1).

Electrochemical properties of MGSI/GC and MGSII/GC electrodes

Electrochemical characteristics of the MGSII/GC electrode in electrolyte solutions

Discussion of the electrochemistry of MGSI/GC and MGSII/GC electrodes requires an idealized model in which a porous film is assumed to be attached to a flat electrode surface. There exist two interfaces, namely, the interface between the substrate and the modifier film and that between the film and the solution. The modifier film must admit ions from the solution or eject ions out of the film in order to maintain the charge balance during the cyclic scanning of the electrode potential. This phenomenon of ion transportation through a film was established in the electrode modified with PB [14–22], in which it was found that the voltammetric response of the modified film depends strongly on the choice of supporting electrolyte. This selective ion permeability in the film was explained in terms of the size of the hydrate ions, the film's channel size, the chemical interaction between the ion and the film, electrostatic factors, the polarizability of cation, etc. [14–22]. The electrochemical response at MGSII/GC in solution containing only 1 M KCl supporting electrolyte was examined. It was found that no peak appeared in the potential range between 700 mV and −800 mV (vs. SCE). We have also examined its electrochemical responses in different electrolyte solutions containing Li^+, Na^+, K^+, Ca^{2+}, Mg^{2+}, Ba^{2+}, Zn^{2+}, Co^{2+}, Ni^{2+}, Mn^{2+}, NH_4^+, Cl^-, NO_3^-, and SO_4^{2-} ions. We did not observe any *I-V* maxima in any of these solutions in the potential range of 700 mV to −800 mV, indicating that the electrochemical reaction in the film was completely blocked. This behavior is different from that observed for PB film [14–22]. The surface voltammetric response of the electrode modified with PB displays a high dependence on the choice of supporting electrolyte and has a high selective ion permeability. It is also different from that observed on the electrode modified with $[CuPtCl_4 \cdot CuPtCl_6]_n$ [33], in which the copper ion acts as the counterion: its admission into and ejection out of the film during the film redox maintains the electroneutrality of the film. The copper ion at the MGSII/GC electrode displays very similar redox behavior to that at a bare GC electrode, indicating that Cu^{2+} does not participate in the formation of the film. We believe that the complete block of the redox process in these electrolyte solutions is due to the lack of exchangeable ions in the film, since both the cation ($Pt(NH_3)_4^{2+}$) and the anion ($PtCl_4^{2-}$ or $PtCl_6^{2-}$) are the building blocks of the polymer's backbone (see Fig. 1). On the other hand, the cations, Cu^{2+} in the $[CuPtCl_4 \cdot CuPtCl_6]_n$ and K^+ in PB, do not participate in the backbones of the film and are therefore exchangeable.

Electrochemical characteristics of H^+ at the MGSII/GC electrode

Similar to the electrode modified by $[CuPtCl_4 \cdot CuPtCl_6]_n$ [33], the MGSII/GC electrode can catalyze the redox of H^+. In order to confirm the redox active species is indeed H^+, we have examined such acids as HCl, H_2SO_4, HNO_3, etc. We found that the responses of all these acidic solutions were identical if the concentrations of H^+ were the same. Some organic acids have also been examined and similar results were obtained, namely, the current response is dependent on the concentration of H^+, not its conjugate anion. Figure 4 shows the redox behavior of H^+ at the MGSII/GC electrode. At a low concentration of H^+ (e.g. 1.5×10^{-3} M HCl), very small and broad redox waves were observed. These broad waves are from the adsorption and desorption of H^+ at the MGSII/GC electrode. This observation is very different from that observed with $[CuPtCl_4 \cdot CuPtCl_6]_n$ film, at which the redox peaks of Pt^{4+}/Pt^{2+} were coupled

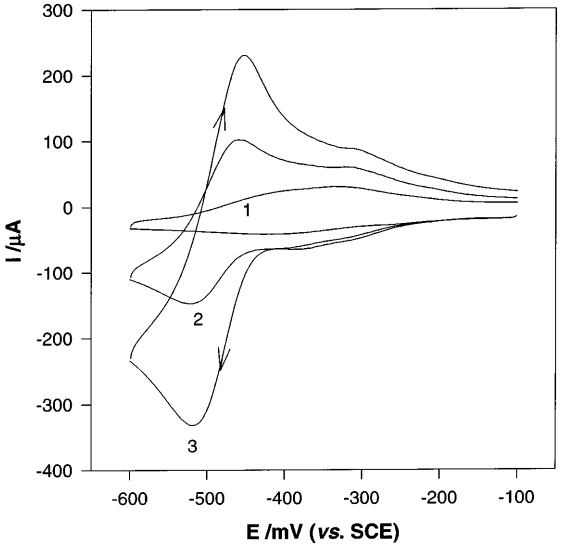

Fig. 4 Cyclic voltammogroms of H^+ at the MGSII/GC electrode. HCl concentrations: (*1*) 1.5×10^{-3}, (*2*) 4.5×10^{-3}, and (*3*) 1.4×10^{-2} M in a solution containing 1 M KCl. Scan rate: 40 mV/s

with the admission and rejection of H^+. This can be understood from the very different structures between $[CuPtCl_4 \cdot CuPtCl_6]_n$ and $[Pt(NH_3)_4 \cdot PtCl_6]_n$ films. In the former, Cu ions do not participate in the structure of the backbone of the polymer. Instead, their role is to serve as the counter ions. Therefore, Cu ions in the film are transportable, and can be substituted by Cu^{2+} and H^+ ions in the solution. In MGSI and MGSII films, both the anion ($PtCl_4^{2-}$ or $PtCl_6^{2-}$) and cation ($Pt(NH_3)_4^{2+}$) participate in the backbone of the polymer, making neither of them a mobile/diffusible species. Therefore, normal cations in the electrolyte solution, such as Cu^{2+} and H^+, are not expected to be admitted into or ejected from the film. When the concentration of H^+ increases, a well-shaped redox couple appeared (traces 2 and 3). The peak currents increase linearly with the increase of H^+ concentration. When the concentration of H^+ is too high ($>1.5 \times 10^{-2}$ M) and the scan rate is too slow (<5 mV/s), the formation H_2 gas was clearly observed, resulting in the current oscillation regulated by the production-desorption of H_2 at the electrode.

In order to understand the redox behavior of H^+ on the MGSII/GC electrode, the effect of scan rate on the current response to H^+ was studied. Figure 5 shows the results obtained from 1.4×10^{-2} M HCl. For comparison purposes, Table 2 summarizes the results obtained from two different H^+ concentrations. The following conclusions can be made from these data. First of all, the peak currents of both the cathodic and the anodic processes exhibit linear relationships with respect to the square root of the scan rate in both H^+ concentrations examined, indicating that the H^+ redox at the MGSII/GC electrode is a diffusion-controlled process. Secondly, the ratio between the peak currents of the cathodic and anodic processes is close to one for all the scan rates and the H^+ concentrations examined, displaying the typical characteristics of a reversible redox process. Thirdly, at the lower scan rate (20 mV/s) and in the lower concentration of H^+ ($\leq 1.4 \times 10^{-2}$ M), the separation of the peak potentials (ΔE_p) is close to the theoretical value (ca. 60 mV) for a diffusion-controlled, single-electron,

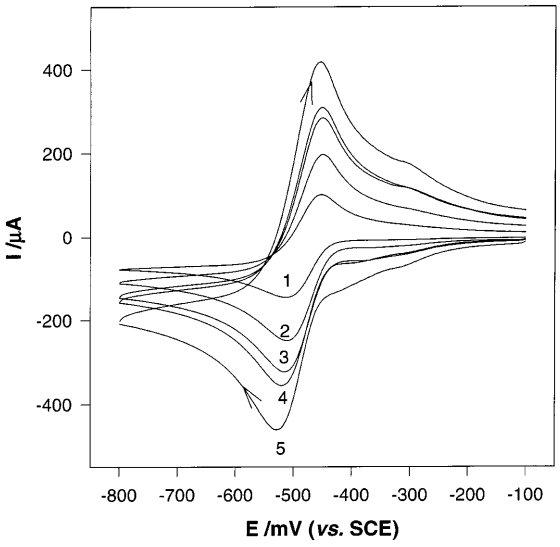

Fig. 5 The effect of scan rate on the response of H^+ at the MGSII/GC electrode: (*1*) 5, (*2*) 20, (*3*) 40, (*4*) 50, (*5*) 100 mV/s, respectively; 1.4×10^{-2} M HCl + 1 M KCl

and reversible redox process. However, the peak potential of the cathodic process shifts to a more negative value and that of the anodic process to a more positive value with increase of the scan rate, resulting in an increase of ΔE with increase of the scan rate. Fourthly, the potential E measured midway between the cathodic and anodic peak potentials, $E = (E_a + E_c)/2$, remains almost a constant at a given H^+ concentration and shifts to a more positive value when the concentration of H^+ increases, in agreement with the tendency predicted by the half-cell formula. All of the experimental evidence that we have obtained so far supports the conclusion that the electrode modified with $Pt(NH_3)_4 \cdot PtCl_6$ can reversibly catalyze the redox of H^+. This process is a H^+ diffusion-controlled, reversible, one-electron redox on the surface of the MGSII/GC electrode. The electrode process can be described as $H^+ + e^- \rightarrow H_{(ad)}$. At a high H^+ concentration and a slow scan rate, the gas

Table 2 The effect of scan rate on the redox behavior of H^+ on a MGSII/GC electrode

C_{H^+} (mol/dm^3)	Scan rate (mV/s)	E_c (mV)	i_{pc} (mA)	E_a (mV)	i_{pa} (mA)	ΔE (mV)	$E = (E_{pa} + E_{pc})/2$	i_{pa}/i_{pc}
1.4×10^{-2}	2	−512	0.094	−454	−0.102	58	−483	1.08
	5	−511	0.159	−453	−0.163	58	−482	1.02
	10	−517	0.201	−456	−0.210	61	−486.5	1.05
	20	−520	0.289	−454	−0.299	66	−487	1.03
	100	−525	0.505	−455	−0.525	70	−490	1.04
	200	−532	0.697	−448	−0.730	84	−490	1.05
	400	−532	0.914	−438	−0.955	94	−485	1.04
	800	−533	1.13	−428	−1.26	104	−480	1.11
5.0×10^{-2}	10	−470	0.781	−403	−0.685	67	−436.5	0.88
	20	−479	1.063	−404	−0.982	75	−441.5	0.92
	40	−489	1.403	−399	−1.279	90	−444	0.91
	100	−509	2.064	−391	−1.994	118	−450	0.97
	200	−527	2.732	−369	−2.524	158	−448	0.92
	400	−552	3.537	−353	−3.320	199	−452.5	0.94
	800	−572	4.562	−332	−4.478	240	−452	0.98

produced at the surface of the electrode is H_2 gas, produced from $H_{(ad)}$.

The redox behavior of Fe^{3+} at the MGSII/GC electrode

Figure 6 shows the typical redox response of Fe(III) at the MGSII/GC electrode in the potential range of 700 mV to −800 mV (vs. SCE). The first redox couple (I_c/I_a) between 400 mV and 200 mV corresponds to the redox of Fe^{3+}. The redox couple (III_c/III_a) between −400 mV and −600 mV corresponds to the redox of protons, as has been already discussed above. The small reduction peak at ~0 mV (II_c) corresponds to the reduction of the dissolved oxygen. When the solution was carefully deaerated prior to measurement, peak II_c disappeared. Here we only focus on the discussion of the redox process of Fe^{3+} (I_c/I_a). It is known that the redox of Fe^{3+} at a bare GC electrode has a large overpotential and is an irreversible process [40]. The redox waves of Fe^{3+} at the MGSII/GC electrode are, however, a very well-shaped and reversible redox couple, as shown in Fig. 6. The following observations can be made for I_c/I_a in Fig. 6. First of all, the peak currents vary linearly with respect to the increase of Fe^{3+} concentration. Therefore, the MGSII/GC electrode provides a convenient probe for the sensitive detection of a trace amount of Fe(III) in a fairly positive potential. Secondly, the ratio of the peak currents between the cathodic and the anodic processes is close to one in all the Fe(III) concentrations examined, suggesting that redox of Fe(III) at the MGSII/GC electrode is indeed a reversible process. Thirdly, the MGSII/GC electrode reduces significantly the redox overpotential of Fe(III) compared with that on the bare GC electrode, and therefore catalyzes the redox of Fe(III). Fourthly, the peak potentials of both the cathodic and anodic processes do not change with the concentration of Fe(III) and ΔE remains almost constant in all the Fe(III) concentrations examined: $\Delta E \approx 112$ mV at the scan rate of 50 mV/s, which is larger than the theoretical value for a one-electron, reversible redox process (60 mV). This may be caused by such kinetic factors as slow electron exchange in the film. Fifthly, the *I-V* curve of Fe(III) at the MGSII/GC electrode was perfectly reproducible when the experiments were carried out continuously for several hours, in contrast to the redox behavior of Fe(III) at a bare GC electrode which is usually not reproducible.

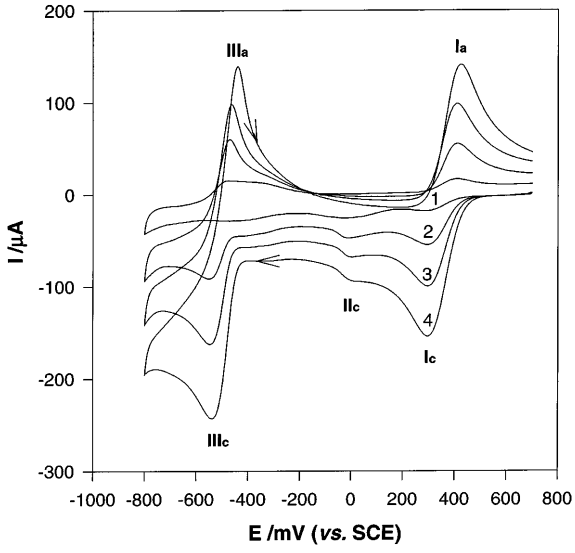

Fig. 6 Cyclic voltammograms of Fe(III) at the MGSII/GC electrode. $FeCl_3$ concentrations (*1*) 2×10^{-3}, (*2*) 5×10^{-3}, (*3*) 1×10^{-2}, and (*4*) 2×10^{-2} M in a solution containing 1 M KCl. Scan rate: 50 mV/s

In order to further understand the nature of the redox reaction of Fe(III) at the MGSII/GC electrode, the effect of scan rate on the current response was measured and the results obtained from 1×10^{-2} M $FeCl_3$ are summarized in Table 3. Several conclusions can be made on the basis of these data. First of all, the ratio I_{pc}/I_{pa} is close to one in all the scan rates examined. Secondly, both I_{pc} and I_{pa} vary linearly with respect to the square root of the scan rate, displaying a typical diffusion-controlled redox process. Thirdly, at the low scan rate (≤10 mV/s), both E_{pc} and E_{pa} as well as ΔE_p remain unchanged with the scan rate. E_{pa} shifts to a more positive value and E_{pc} shifts to a more negative value when the scan rate increases further (>10 mV/s), resulting in an increase of ΔE_p. However, the midway potential $E = (E_a + E_c)/2$ remains almost a constant, except at very fast scan rates (>200 mV/s) when the midway potential shifts to a more negative value.

From these discussions, we can conclude that the MGSII/GC electrode catalyzes efficiently and reversibly the redox reaction of $Fe^{3+/2+}$, which can be described as $Fe^{3+} + e^- \rightleftharpoons Fe^{2+}$. Moreover, the charge propagation through the modifier film does not seem to limit the net reaction rate. The MGSII/GC electrode can therefore be employed as a sensitive and quantitative detector for the measurement of trace amounts of Fe(III).

Table 3 The effect of scan rate on the redox behavior of 1×10^{-2} M Fe(III) on a MGSII/GC electrode

Scan rate (mV/s)	E_c (mV)	i_{pc} (μA)	E_a (mV)	i_{pa} (μA)	ΔE (mV)	$E = (E_{pa} + E_{pc})/2$	i_{pa}/i_{pc}
5	323	36.77	408	−34.17	85	365.5	0.93
10	323	45.58	407	−46.84	84	365	1.03
20	320	62.25	418	−65.07	98	369	1.04
40	313	84.52	420	−89.39	107	366.5	1.06
100	296	129.5	428	−135.2	132	362	1.04
200	282	168.6	434	−187.2	152	358	1.10
400	259	232.0	445	−251.3	186	352	1.08

The redox behavior of Cr^{3+} at the MGSII/GC electrode

The cyclic voltammograms of Cr(III) at the bare GC (curve 1) and the MGSII/GC (curve 2) electrodes are shown in Fig. 7. For this particular experiment, a solution containing 1×10^{-2} M of $CrCl_3$ and a scan rate of 100 mV/s were used. While no peak current was observed for Cr(III) on the bare GC (curve 1), quite complicated redox processes took place on MGSII/GC in the scanned potential range. The complexity of the CV is because the redox waves of Cr(III) appeared at similar positions to that of the H^+ (see Fig. 4). It is known that aqueous Cr(III) solution is usually quite acidic owing to hydrolysis of the hydrated Cr(III) ion. The electrode reaction of Cr(III) itself on MGSII/GC can be described as $Cr^{3+} + e^- \rightarrow Cr^{2+}$. The peak currents increased with the increase of Cr^{3+} concentration.

The effect of scan rate on the response to Cr^{3+} at the MGSII/GC electrode shows that the peak currents increase linearly with respect to the square root of the scan rate for both the cathodic and the anodic processes, and that the I_{pa}/I_{pc} ratio is close to one, and the E_{pa} and E_{pc} are also affected by the scan rate in a similar manner as that of Fe(III). ΔE_p is much larger than the theoretical value for a reversible, one-electron redox process, even at a very slow scan rate. From these results we can conclude that the redox reaction of Cr^{3+} on the MGSII/GC electrode is a diffusion-controlled, quasi-reversible process.

Electrocatalytic behavior of the MGSII/GC electrode

Platinum metal and its various ion complexes have been widely used as catalysts for various chemical transformations. We therefore examined the electrocatalytic activities of the MGSII/GC electrode with several analytes, and the results are summarized below.

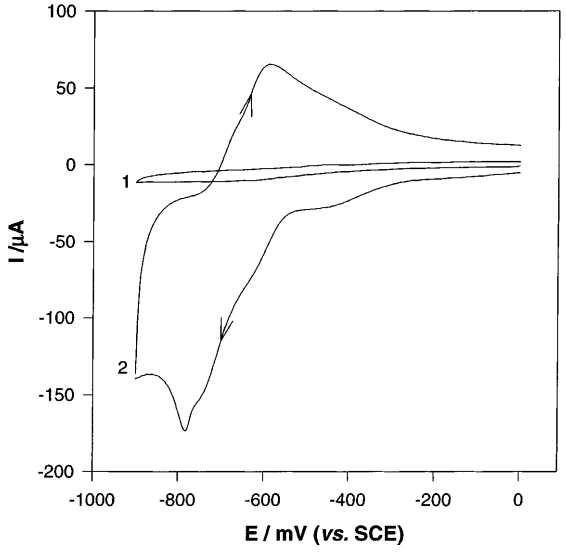

Fig. 7 Cyclic voltammograms of Cr(III) on *1* GC and *2* MGSII/GC electrodes in 1×10^{-2} M $CrCl_3 + 1$ M KCl. Scan rate: 50 mV/s

Electrocatalytic oxidation of ascorbic acid

Figure 8 shows the cyclic voltammograms of 4×10^{-3} M ascorbic acid on a bare GC (curve 1) and MGSII/GC (curve 2) electrodes, respectively. The oxidation peak of ascorbic acid appeared at about 500 mV (vs. SCE) on the surface of the bare GC electrode and has a very broad *I-V* voltammogram, indicating a slow and heterogeneous electron-transfer rate at the bare GC substrate. The peak current for the oxidation of ascorbic acid on the MGSII/GC electrode appears at around 250 mV, displaying a decrease of the overpotential by nearly 250 mV. The peak shape improved dramatically and the oxidation current increased markedly compared with that on bare GC. Further experiments showed that the peak current for the oxidation of ascorbic acid on MGSII/GC is linearly proportional to its concentrations over a very wide range (5 μM to 1 mM), providing a promising electrochemical detector for the detection of ascorbic acid. It should be pointed out that the redox peaks at around −400 mV in curve 2 of Fig. 8 are due to the redox of H^+ in the solution.

Electrocatalytic oxidation of $S_2O_3^{2-}$

Figure 9 shows the cyclic voltammograms obtained on the bare GC (curve 1) and MGSII/GC (curve 2) electrodes in a solution containing 5×10^{-3} M $Na_2S_2O_3$ + 1 M KCl. The comparison of the two CV currents suggests clearly that the MGSII/GC electrode has a remarkable catalytic effect on the oxidation of $S_2O_3^{2-}$. The catalytic oxidation of $S_2O_3^{2-}$ at MGSII/GC peaks at ca. 550 mV, and varies linearly with respect to the $S_2O_3^{2-}$ concentration. This result demonstrates that the MGSII film acts as a good electrocatalyst for the

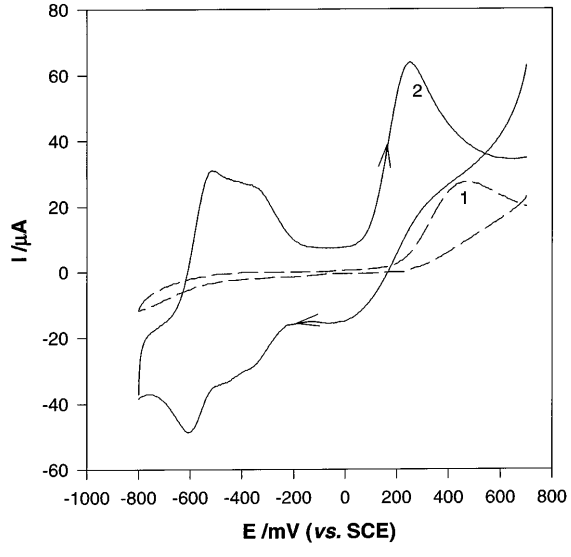

Fig. 8 Cyclic voltammograms of ascorbic acid on *1* GC and *2* MGSII/GC electrodes in 4×10^{-3} M ascorbic acid + 1 M KCl. Scan rate: 50 mV/s

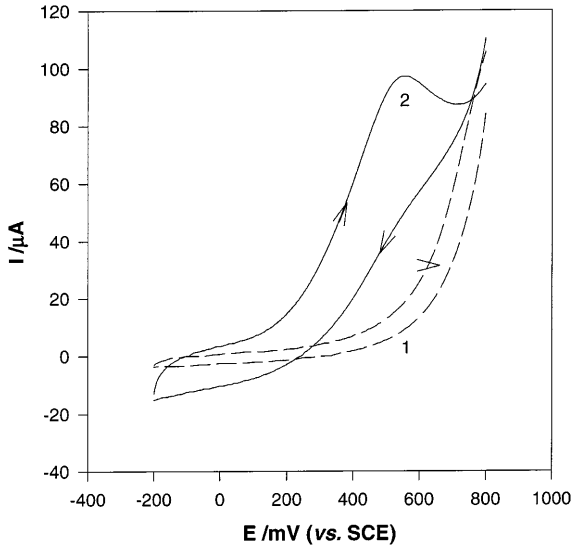

Fig. 9 Cyclic voltammograms of $S_2O_3^{2-}$ on *1* GC and *2* MGSII/GC electrodes in 5×10^{-3} M $Na_2S_2O_3$ + 1 M KCl. Scan rate: 100 mV/s

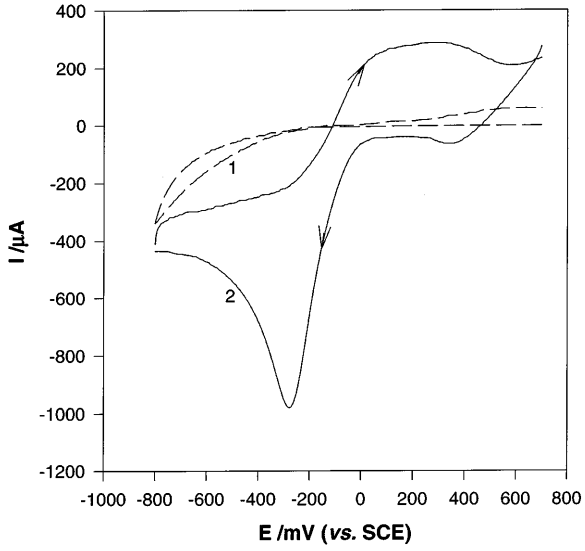

Fig. 10 Cyclic voltammograms at *1* bare GC and *2* MGSII/GC electrodes in 5×10^{-3} M H_2O_2 + 1 M KCl. Scan rate: 100 mV/s

oxidation of $S_2O_3^{2-}$, and therefore provides a convenient probe for the detection of $S_2O_3^{2-}$.

Electrocatalytic activity and redox of H_2O_2

The electrocatalytic effect of the MGSII/GC electrode on the redox of H_2O_2 is shown in Fig. 10. No obvious current peak due to H_2O_2 appeared on the bare GC electrode (curve 1) in the scanned potential range. However, remarkably enhanced peak currents for H_2O_2 appeared on both the cathodic and the anodic processes at MGSII/GC (curve 2). The reduction peak at −300 mV is particularly impressive because of its well-shaped profile and its remarkable intensity, which provides an excellent probe for the quantitative and selective detection of H_2O_2.

Electrocatalytic oxidation of NO

Nitric oxide, a diatomic and free radical-like molecule, has been established recently as one of the important cellular messenger molecules in human physiology. Therefore, there have been strong demands for the measurement of NO release in biomedia in a selective, sensitive, and quantitative manner [41]. Both our MGSII/GC and MGSI/GC electrodes display very good electrocatalytic activity for the oxidation of NO. Figure 11 shows the cyclic voltammograms obtained on the bare GC (curve 1) and MGSII/GC (curve 2) electrodes, respectively, in a solution containing 8×10^{-5} M NO + 1 M KCl. A broad and very weak oxidation current at much more positive potential (+900 mV vs. SCE) was observed on the bare GC electrode. However, a remarkably enhanced anodic current appears on the MGSII/GC electrode at a potential of ca. 790 mV. This

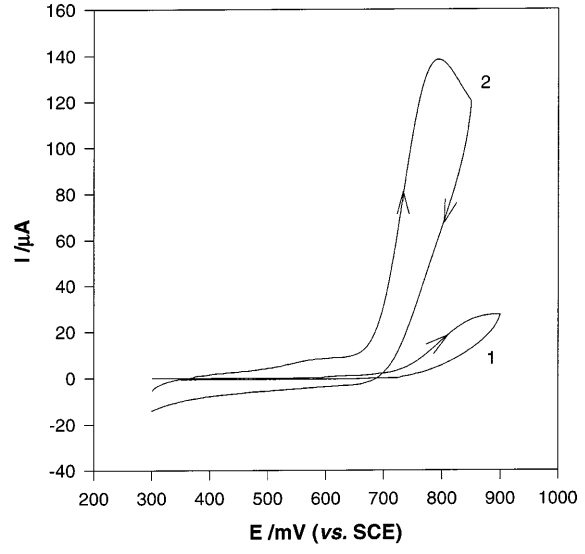

Fig. 11 Cyclic voltammograms at *1* bare GC and *2* MGSII/GC electrodes in 8×10^{-5} M NO + 1 M KCl. Scan rate: 50 mV/s

oxidation current displays an excellent linear relationship with respect to the concentration of NO from 1×10^{-8} to 2×10^{-4} M in amperometry mode. The application of an ultramicroelectrode modified with MGSI and MGSII for the detection of NO is in progress.

Conclusions

Electrodes chemically modified with electropolymerized MGS, $[Pt(NH_3)_4 \cdot PtCl_4]_n$ and $[Pt(NH_3)_4 \cdot PtCl_6]_n$, have been successfully prepared by cyclic scanning of the potential at the working electrode in solutions containing $Pt(NH_3)_4^{2+}$ and $PtCl_6^{2-}$ or $PtCl_4^{2-}$ ions. The films can

be electrodeposited on either a GC electrode or on a Pt or Au substrate. The conditions for the electrodeposition of the film have been examined in detail. Several surface analysis techniques, including Raman scattering, XRD, and electrochemical characteristics, have been employed to characterize the modifier film. It is shown that the film was grown electrochemically with a highly preferred orientation, along the alternative cation-anion stacking axis. The electrochemical behavior of the modified electrodes were studied in detail in electrolyte solutions containing various cations. H^+, Fe^{3+}, and Cr^{3+} ions exhibit reversible electrochemical behavior at the modified electrode. The modified electrode displays very good electrocatalytic activity toward ascorbic acid, H_2O_2, $S_2O_3^{2-}$, and especially nitric oxide. The application of an ultramicroelectrode modified with MGS for the detection of biological nitric oxide is in progress.

Acknowledgements We acknowledge the support of this project by the Research Grant Council of Hong Kong and by The Hong Kong University of Science and Technology.

References

1. Murray RW (1984) Chemically modified electrodes. In: Bard AJ (ed) Electroanalytical chemistry, vol. 13. Dekker, New York, pp 191–368
2. Inzelt G (1994) Mechanism of charge transport in polymer-modified electrode. In: Bard AJ (ed) Electroanalytical chemistry, vol. 18. Dekker, New York, pp 89–241
3. Abruña HD (1988) Coord Chem Rev 86: 135
4. Diaz AF, Rubinson JF, Mark HB (1988) Adv Polym Sci 84: 113
5. Wang B, Dong S (1994) J Electroanal Chem 154: 207
6. Keita B, Nadjo L (1989) J Electroanal Chem 269: 447
7. Malinski T, Taha Z (1992) Nature 358: 676
8. Coutanceau C, Rakotondrainibe A, Crouigneau P, Léger JM, Iamy C (1995) J Electroanal Chem 386: 173
9. Moyer BA, Thompson MS, Meyer TJ (1980) J Am Chem Soc 102: 2310
10. Shen PK, Chen KY, Tseung ACC (1995) J Electroanal Chem 389: 223
11. Casella IG, Cataldi TRI, Salvi AM, Desimoni E (1993) Anal Chem 65: 3143
12. Xie Y, Hubber CO (1991) Anal Chem 63: 1714
13. Wang J, Taha Z (1990) Anal Chem 62: 1413
14. Neff VD (1978) J Electrochem Soc 125: 886
15. Ellis D, Eckhoff M, Neff VD (1981) J Phys Chem 85: 1225
16. Kuhnhardt C (1994) J Electroanal Chem 369: 71
17. Sperko LM, Kuwana T (1983) J Electrochem Soc 130: 396
18. Itaya K, Shoji N, Uchida I (1984) J Am Chem Soc 106: 3423
19. Jiang M, Zhao Z (1990) J Electroanal Chem 292: 281
20. Zakharchuk NF, Meyer B, Henning H, Scholz F (1995) J Electroanal Chem 398: 23
21. Dostal A, Meyer B, Scholz F (1995) J Phys Chem 99: 2096
22. Dostal A, Kauschka G, Reddy SJ, Scholz F (1996) J Electroanal Chem 406: 155
23. Anson FC, Oshaka T, Saveant JM (1983) J Am Chem Soc 105: 4883
24. Miller JS, Epstein AJ (1976) One-dimensional inorganic complexes. In: Lippard SJ (ed) Progress in inorganic chemistry, vol 20. Wiley, New York, pp 1–151
25. Kamata T, Fukaya T, Mizuno M, Matsuda H, Mizukami F (1994) Chem Phys Lett 221: 194
26. Kimura N, Ohki H, Ikeda R, Yamashita M (1994) Chem Phys Lett 220: 40
27. Scrocco M (1991) Phys Rev B 44: 1337
28. Miller JS (1976) Science 194: 189
29. Saillant RB, Jaklevic RC, Bedford CD (1974) Mater Res Bull 9: 289
30. Guggenheim HJ, Bahnck D (1974) J Crystal Growth 26: 29
31. Williams JM, Gerrity DP, Schultz AJ (1977) J Am Chem Soc 99: 1668
32. Ward MD (1989) Electrochemical aspects of low-dimensional molecular solids. In: Bard AJ (ed) Electroanalytical chemistry, vol 16. Dekker, New York, pp 181–312
33. Pei JH, Li XY (1998) J Electroanal Chem 441: 245
34. Honda K, Chiba K, Tsuchida E, Frank AJ (1989) J Mater Sci 24: 4004
35. Awano H, Sakai S, Kuriyama T, Ohba Y (1994) Bull Chem Soc Jpn 67: 1737
36. Ferraro JR (1979) Coord Chem Rev 29: 1
37. Nakamoto K (1986) Infrared and Raman spectra of inorganic and coordination compounds. Wiley, New York
38. Manfait M, Alix AJP, Bernard L, Theophanides T (1978) J Raman Spectrosc 7: 143
39. Schneider H (1931) Z Anorg Chem 202: 79
40. Kulesza PJ, Brajter K, Dabek-Zlotorzynska E (1987) Anal Chem 59: 2776
41. Bedioui F, Trevin S, Devynck J (1996) Electroanalysis 8: 1085